JACS Au
AN OPEN ACCESS JOURNAL OF THE AMERICAN CHEMICAL SOCIETY

pubs.acs.org/jacsau
Article

A "One-Step" Strategy for the Global Characterization of Core-Fucosylated Glycoproteome

Yuqiu Wang,◆ Rui Yuan,◆ Bo Liang,◆ Jing Zhang, Qin Wen, Hongxu Chen, Yinping Tian,* Liuqing Wen,* and Hu Zhou*

Cite This: JACS Au 2024, 4, 2005−2018
Read Online

ACCESS | Metrics & More | Article Recommendations | Supporting Information

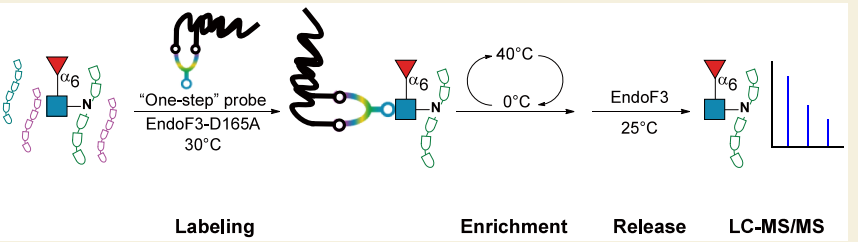

ABSTRACT: Core fucosylation, a special type of *N*-linked glycosylation, is important in tumor proliferation, invasion, metastatic potential, and therapy resistance. However, the core-fucosylated glycoproteome has not been extensively profiled due to the low abundance and poor ionization efficiency of glycosylated peptides. Here, a "one-step" strategy has been described for protein core-fucosylation characterization in biological samples. Core-fucosylated peptides can be selectively labeled with a glycosylated probe, which is linked with a temperature-sensitive poly(*N*-isopropylacrylamide) (PNIPAM) polymer, by mutant endoglycosidase (EndoF3-D165A). The labeled probe can be further removed by wild-type endoglycosidase (EndoF3) in a traceless manner for mass spectrometry (MS) analysis. The feasibility and effectiveness of the "one-step" strategy are evaluated in bovine serum albumin (BSA) spiked with standard core-fucosylated peptides, H1299, and Jurkat cell lines. The "one-step" strategy is then employed to characterize core-fucosylated sites in human lung adenocarcinoma, resulting in the identification of 2494 core-fucosylated sites distributed on 1176 glycoproteins. Further data analysis reveals that 196 core-fucosylated sites are significantly upregulated in tumors, which may serve as potential drug development targets or diagnostic biomarkers. Together, this "one-step" strategy has great potential for use in global and in-depth analysis of the core-fucosylated glycoproteome to promote its mechanism research.

KEYWORDS: *glycosylation, glycoproteomics, core-fucosylation, chemoenzymatic labeling, one-step strategy, lung adenocarcinoma, biomarker*

INTRODUCTION

Protein glycosylation (*N*-linked, *O*-linked, or *C*-linked) is one of the most ubiquitous and complex posttranslational modifications (PTMs), which is involved in various biological processes.[1,2] Core fucosylation is a special type of *N*-linked glycosylation, in which α1,6-fucose residue attaches to the innermost *N*-acetylglucosamine (GlcNAc) residue of *N*-linked glycans.[3] The formation of core fucosylation is catalyzed by a single enzyme_fucosyltransferase 8 (FUT8) in humans.[4] Emerging evidence indicates that core fucosylation is associated with inflammation and cancer aggressiveness.[5] An aberrant increase in core fucosylation is observed during tumorigenesis in various cancers, such as hepatocellular carcinoma (HCC), non-small-cell lung cancer (NSCLC), pancreatic ductal adenocarcinoma (PDAC), etc.[6−8] Many studies indicate that increased core fucosylation promotes proliferation, invasion, metastatic potential, and therapy resistance.[9−11] The core-fucosylated alpha-fetoprotein (AFP) has been approved by the Food and Drug Administration (FDA) as a clinical HCC diagnostic marker. It is worth noting that the increase in core-fucosylated AFP in HCC patients can indicate cancer progression more specially than the increase in total AFP.[12] Recently, another interesting discovery by Zhang and coworkers showed that multiple viral envelop proteins, such as hepatitis C virus (HCV)-E2 and severe acute respiratory syndrome coronavirus 2 (SARS-CoV-2)-spike, enhance FUT8 expression and core fucosylation levels.[13] As a consequence, the development of efficient strategies to identify and quantify aberrant core fucosylation would provide a means for the discovery of new drug targets or diagnostic biomarkers.

Received: March 6, 2024
Revised: April 21, 2024
Accepted: April 22, 2024
Published: May 1, 2024

https://doi.org/10.1021/jacsau.4c00214
JACS Au 2024, 4, 2005−2018

Scheme 1. A "One-Step" Probe for the Global Profiling of Core-Fucosylated Glycoproteome

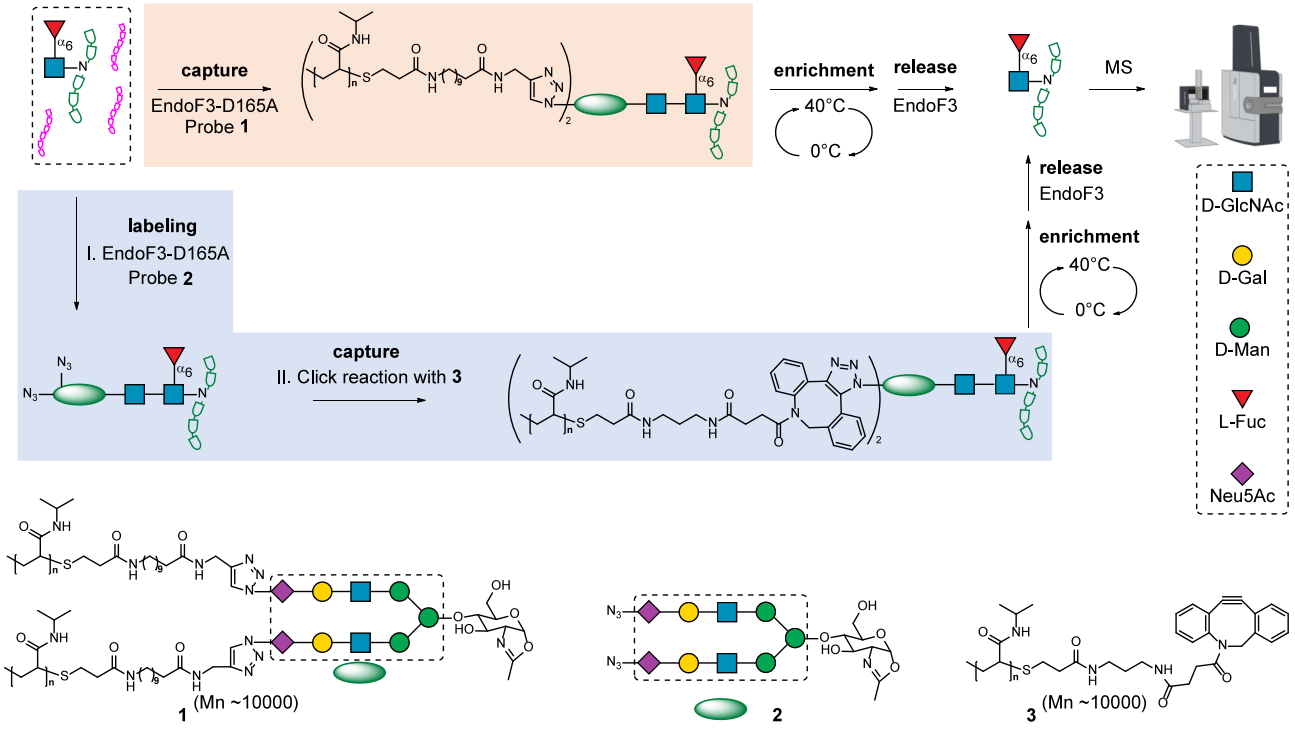

Due to the low abundance and poor ionization efficiency of glycosylated peptides, the detection of core-fucosylated sites in complex mixtures is challenging. To improve the coverage of core-fucosylated sites, it is essential to efficiently isolate core-fucosylated peptides from the digests of complex mixtures. Currently, diverse strategies have been developed for the enrichment of core-fucosylated peptides before liquid chromatography with tandem mass spectrometry (LC-MS/MS) analysis, such as lectin binding,[14,15] hydrophilic interaction chromatography (HILIC),[16,17] mixed-mode polymeric sorbent,[18,19] metabolic labeling,[20,21] and chemoenzymatic labeling.[22,23] Lectin binding is widely used for purifying core-fucosylated peptides, owing to its affordability and ease of use. However, this method often suffers from weak binding affinity, cross reactivity, and waste of time.[24] Recently, chemoenzymatic labeling has been developed to profile core fucosylation for its good specificity and few side reactions.[22,23,25] There are two types of probes that have been widely used in chemoenzymatic labeling methods namely "two-step probes" and "one-step probes."[26] A "two-step probe" contains a biorthogonal reactive group, such as an alkynyl or azido group, and additional chemical reactions are required to introduce a reporter group. In contrast, a "one-step probe" is conjugated with a reporter group, such as a fluorescent or biotin group, via a covalent bond. Accumulating evidence shows that the "one-step probe" is much more sensitive than the "two-step probe" as it only relies on the enzymatic transfer and does not need additional chemical reaction.[27−29] These results have encouraged us to develop a "one-step" strategy for the global characterization of core-fucosylated glycoproteome in complex mixtures.

In this work, a "one-step" strategy is described for protein core-fucosylation characterization in biological samples. Core-fucosylated peptides from complex biological samples were selectively labeled with a glycosylated probe (**1**), which is linked with a temperature-sensitive poly(*N*-isopropylacrylamide) (PNIPAM) polymer, by mutant endoglycosidase (EndoF3-D165A) (Scheme 1). The tagged probes can be reversibly removed by wild-type endoglycosidase (EndoF3) in a traceless manner for LC-MS/MS analysis. The performance of "one-step" strategy was evaluated in bovine serum albumin (BSA) spiked with standard core-fucosylated peptides, H1299, and Jurkat cell lines. Finally, the "one-step" strategy was applied to characterize core-fucosylated sites in human lung adenocarcinoma (LUAD).

RESULTS AND DISCUSSION

Enrichment methods are often required before LC-MS/MS analysis, as core fucosylation has a low abundance in cells. Recently, we have developed a reversible labeling strategy for core fucosylation analysis on cell surface by using a biotinylated probe and EndoF3-D165A from *Elizabethkingia meningoseptica*.[22] Nevertheless, this strategy cannot be used to label cell lysates or human samples as a strong nonspecific labeling signal caused by the oxazoline group was observed. Therefore, we have developed a "two birds one stone" method for core-fucosylated peptides and *O*-GlcNAcylated peptides analysis by employing a temperature sensitive PNIPAM.[23] This method depended on a "two-step" enrichment strategy. First, mutant endoglycosidase (EndoF3-D165A) added an oxazoline probe (**2**) bearing an azido group to the target glycopeptides, and then the azido modified glycopeptides were linked with dibenzocyclooctyne functionalized PNIPAM (**3**) through strain-promoted azide−alkyne cycloaddition (SPAAC) reaction. Following a temperature dependent enrichment process, the target glycopeptides were enriched and released with wild-type endoglycosidase (EndoF3) for LC-MS/MS analysis. These two works indicated that endoglycosidases are powerful tools for glycosylation study. Inspired by these works, we developed a glycosylated probe (**1**) for efficient enrichment of

https://doi.org/10.1021/jacsau.4c00214
JACS Au 2024, 4, 2005−2018

core fucosylation in a "one-step" manner and in-depth site-specific analysis in large scale (Scheme 1).

Synthesis and Characterization of Probe 1

PNIPAM (Mn ∼ 10 000), a temperature-sensitive polymer of *N*-isopropylacrylamide, displays an outstanding water solubility at room temperature, resulting in excellent compatibility with enzyme-catalyzed reactions. Therefore, a glycosylated probe (**1**) was synthesized by combining glycans (precursor of the enzymatic substrate) with PNIPAM via a hydrophobic linker. The alkyne modified linker (**8**) was prepared from 11-((*tert*-butoxycarbonyl)amino)undecanoic acid (**6**) through two step reactions. An alkyne linker bearing an amino group was reacted with carboxylated PNIPAM (**9**) and was linked with azido-modified glycans (**10**) through a copper-catalyzed azide–alkyne cycloaddition reaction to give glycosylated polymer **11**. Probe **1** was obtained by treating **11** with 2-chloro-1,3-dimethylimidazolinium chloride (DMC) in the presence of triethylamine (Scheme 2, Figure S1; for synthesis details, see

Scheme 2. Chemical Synthesis of Probe 1

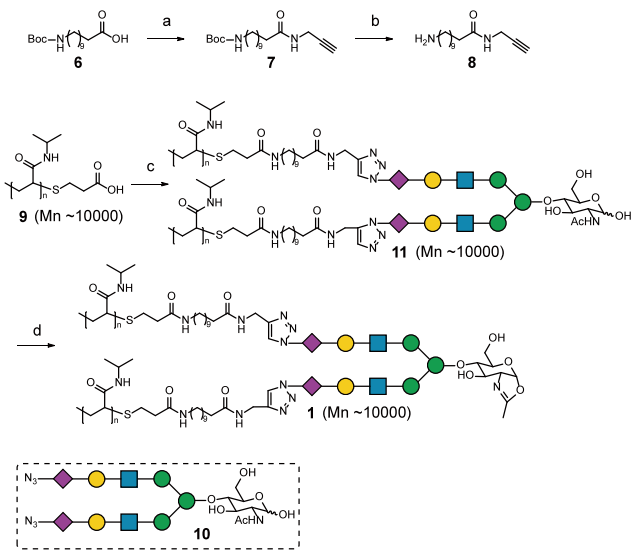

a) prop-2-yn-1-amine, HATU, DIPEA, DCM, 80%; b) 50% TFA/DCM, 86%; c) i) **8**, HATU, DIPEA, DMF, ii) $CuSO_4$, VcNa, THPTA, **10**, H_2O, 53% for two steps; d) DMC, Et_3N, H_2O, quantitative.

the Materials and Methods). Compound **1** bearing an oxazoline group was a donor of EndoF3-D165A and could be added to core-fucose (Fucα1,6GlcNAc structure) modified substrates through enzyme-catalyzed reaction.

The Enrichment Effectiveness of a Core-Fucosylated Peptide with Two Strategies

A core-fucosylated peptide (**4**) was enriched with two strategies following the procedure described in Scheme 1, respectively. For the "one-step" procedure, probe **1** was added to the solution of **4** for three times every 1 h in the presence of EndoF3-D165A to capture **4**. For the "two-step" procedure, probe **2** was added to the solution of **4** for five times every 0.5 h in the presence of EndoF3-D165A to produce an azido-peptide (**5**). **5** was linked with compound **2** at room temperature for 1 h. Then, the temperature of the above mixtures was raised to 40 °C to precipitate the PNIPAM compounds. After centrifugation, the supernatant was analyzed by HPLC to obtain the decrease of the core-fucosylated peptide (after enrichment with **1**) or the azido peptide (after enrichment with **3**). The precipitate was washed to remove unreacted compounds and incubated with wild-type EndoF3 to release the enriched glycopeptide (**4**). HPLC analysis showed that **4** could be effectively enriched with probe **1**, indicating that glycosylated polymer **1** can be accepted by EndoF3-D165A (Figure 1A). Furthermore, the enriched core-fucosylated peptide was well released from probes **1** and **3**. This is due to excellent substrate tolerance of EndoF3-D165A and EndoF3 and the PNIPAM polymer's outstanding compatibility with enzymatic reactions in aqueous solutions.[30,31]

Next, we compared the effectiveness of two strategies in enriching the core-fucosylated peptide from a mixture of core-fucosylated peptides and BSA digests. Core-fucosylated peptide **4** was mixed with trypsin-digested peptides from BSA at a ratio of up to 1:500 (w/w). The mixture was enriched as described above using probe **1** or probes **2** and **3**, respectively. After intensive washes, the captured core-fucosylated peptide was released with EndoF3 and analyzed by MS. It was difficult to identify the peak of core-fucosylated peptide in the original mixture by MS as it was merged with other signals. After the enrichment procedure, the target peaks became dominant (Figures 1B and S2). Then, we calculated the peak area of the target glycopeptide (**4**) to evaluate the effectiveness of the two probes. The peak area of **4** after enrichment by probe **1** was approximately 1.9 times greater than that after enrichment by probes **2** and **3** (Figure 1C). The further LC-MS/MS analysis gave information on where the glycosylation site occurred (Figure 1D). These findings indicate that probe **1** is more effective than probes **2** and **3** for performing site-specific analysis of core fucosylation in a mixture of core-fucosylated peptides and BSA digests.

Identification of Core-Fucosylated Sites in Human Cell Lines

We next employed probe **1** and probes **2** and **3** to profile the core-fucosylated glycoproteome in two human cancer cell lines, a lung cancer cell line (H1299) and a lymphocyte cell line (Jurkat). Proteins (10 mg) extracted from cancer cells were digested into peptides by trypsin. The peptide mixture (3 mg) was treated with EndoF3 to expose the reactive group (Fucα1,6GlcNAc structure) before the labeling reaction. The peptide mixture was labeled and enriched as described above. After intensive washing, the captured glycopeptides were released from the PNIPAM polymers (**1** and **3**) by EndoF3. In total, approximately 9.4 μg (0.31%) of glycopeptides was obtained using probe **1**, whereas about 7.5 μg (0.25%) of glycopeptides was obtained using probes **2** and **3**. Owing to the better enrichment effectiveness of probe **1**, more glycopeptides was obtained. The enriched glycopeptides were further fractionated into six fractions with a tip-based concatenated high-pH reversed phase to improve the coverage of core fucosylation analysis. The fractionated peptides were analyzed by LC-MS/MS, and the MS data were processed by MaxQuant software.[32] The identified core-fucosylated sites were considered positive results only if they occurred at the consensus motif of N-X-S/T/C (X ≠ P).

In H1299, 1200 core-fucosylated sites corresponding to 652 glycoproteins and 828 core-fucosylated sites corresponding to 491 glycoproteins were identified by using probe **1** and probes **2** and **3**, respectively (Figure 2A and Table S1). Almost all of the core-fucosylated sites (95.7%) identified by using probes **2**

https://doi.org/10.1021/jacsau.4c00214
JACS Au 2024, 4, 2005−2018

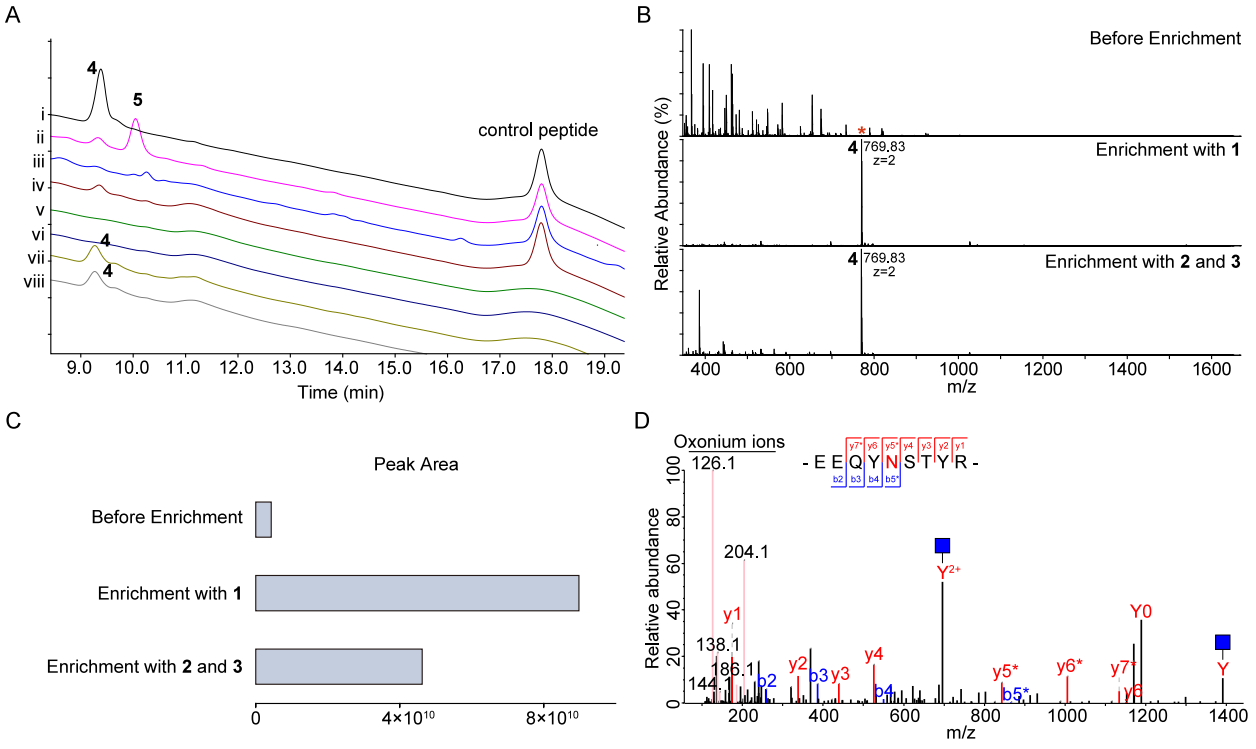

Figure 1. Enrichment and detection of core-fucosylated peptide (**4**) by the "one-step" and "two-step" methods. (A) HPLC analysis of the "catch and release" process of **4** following the procedure shown in Scheme 1. (i) HPLC profile of standard glycopeptide **4** and control peptide. (ii) Glycopeptide **4** and control peptide were incubated with probe **2** and EndoF3-D165A at 30 °C for 2.5 h to produce azido-peptide **5**. (iii) Supernatant of the reaction after enrichment of **4** with probe **1** by centrifugation. (iv) Supernatant of the reaction after enrichment of **5** with probe **3** by centrifugation. (v,vi) Supernatant of the control group (only containing the enriched polymers **1** and **3**). (vii,viii) Release of the glycopeptides from the enriched polymers **1** and **3** by EndoF3, respectively. During the repeat experiments, the peptide peaks were further collected and confirmed by MS analysis (see the Materials and Methods for experimental details). (B) Mass spectra and (C) peak area of LC−MS analysis of the glycopeptide (**4**) and BSA peptide mixture (w/w 1:500) before and after enrichment by the "one-step" (probe **1**) and "two-step" (probes **2** and **3**) methods. The red asterisk indicates glycopeptide (**4**). (D) HCD MS/MS spectrum of the released glycopeptides.

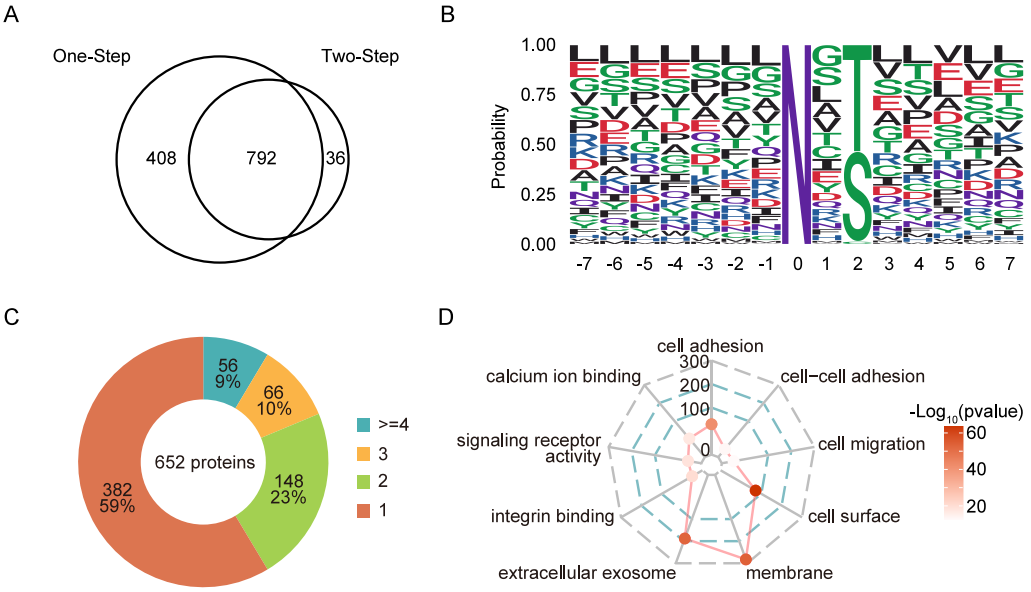

Figure 2. Core-fucosylated sites identified by the "one-step" (probe **1**) method in H1299 cells. (A) Overlapped core-fucosylated sites identified by "one-step" (probe **1**) and "two-step" (probes **2** and **3**) methods. (B) Motif alignment of amino acids adjacent to core-fucosylated sites. (C) Distribution of core-fucosylated sites. (D) Clustering of identified core-fucosylated proteins based on the biological process, cellular component, and molecular function.

and **3** were detected by using probe **1**. The motif of the core-fucosylated sites showed that T was more frequently found in position 2 compared to S with a frequency rate of 53.5% (probe **1**) and 54.2% (probes **2** and **3**), which was in

https://doi.org/10.1021/jacsau.4c00214
JACS Au 2024, 4, 2005−2018

accordance with the previous report (Figures 2B and S3A).[33] The distribution of core-fucosylated sites on proteins was also investigated, and at least 9% (probe **1**) and 7% (probes **2** and **3**) of the proteins had more than four sites (Figures 2C and S3B). Protein clustering results showed that the identified core-fucosylated proteins were mainly enriched in the biological processes of cell adhesion and cell migration, the cellular components of membrane and extracellular exosome, and the molecular functions of integrin binding and signaling receptor activity (Figures 2D and S3C). In Jurkat, 1277 core-fucosylated sites corresponding to 694 glycoproteins and 951 core-fucosylated sites corresponding to 550 glycoproteins were identified by employing probe **1** and probes **2** and **3**, respectively (Figures S4 and S5 and Table S2). These results indicated that probe **1** showed better enrichment effectiveness of core-fucosylated sites from human cell lines and could promote core fucosylation analysis from complex samples.

In total, 1236 core-fucosylated sites corresponding to 671 glycoproteins and 1345 core-fucosylated sites corresponding to 722 glycoproteins were identified in H1299 and Jurkat in this work (Figure S6). The function and domain of these glycoproteins were similar between H1299 and Jurkat, which was consistent with previous reports (Figures S7–S9).[16,17,22] Notably, up to 785 core-fucosylated sites were overlapped in the two cell lines, and these conservative glycosylated sites potentially play essential roles in cellular function as the evolutionary selection (Table S3). In our previous work, 119 conservative core-fucosylated sites were identified in HepG2, MCF7, and HeLa, 99 (83.2%) of which were detected in this work (Figure S6). These results indicated the high coverage and confidence of the core fucosylation in this work. Then, the relative position of the 785 conservative sites in protein sequence was plotted and showed that proteins prolow-density lipoprotein receptor-related protein 1 (LRP1) and insulin-like growth factor 2 receptor (IGF2R) had the highest number of conservative sites reaching 18 and 13 sites with distinct peptide sequences surrounding the sites (Figure S10). These heavily core-fucosylated proteins were reported to be associated with cancer invasion.[34,35] Furthermore, it was observed that these 785 sites had relatively even distribution across the protein sequence but less frequent at the protein C-terminus (Figure S10). This was in accordance with previous studies that the glycosylation efficiency of N-X-S/T/C (X ≠ P) motif decreases toward the C terminus.[36,37]

Mapping Aberrant Core-Fucosylated Sites Associated with Human LUAD

LUAD is one of the most common and fatal lung cancers in the world.[38] Here, we performed proteomic and "one-step" method-based core-fucosylated glycoproteomic analysis of 4 pairs of LUAD tumors and normal adjacent tissues (NATs). This analysis of tumors and NATs was performed at the same time to ensure a similar enrichment recovery bias between tumors and NATs. A total of 2494 core-fucosylated sites (2371 sites in tumors; 2161 sites in NATs) corresponding to 1176 glycoproteins were identified (Figure 3A and Table S4). The abundance of these glycoproteins was further investigated, and it was observed that many glycoproteins with low abundance could also be identified by the "one-step" (probe **1**) method (Figure 3B). The motif, distribution, and function of these core-fucosylated proteins were similar to that of glycoproteins in cell lines (Figures S11 and S12). However, owing to the complexity of tissue samples, about two-thirds of core-fucosylated sites detected in cell lines were also identified in the LUAD sample (Figure S13A). The results from cell lines and LUAD sample were combined, 3081 core-fucosylated sites were identified in this work, and approximately 61.7% (1900 sites) were newly identified (Figure S13B).

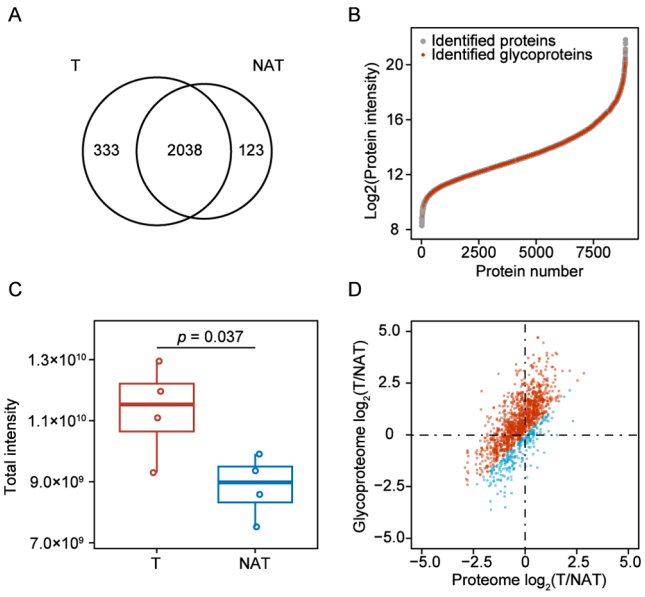

Figure 3. Profiling of core fucosylation in human LUAD by the "one-step" (probe **1**) method. (A) Number of identified core-fucosylated sites in tumors and the paired NATs. (B) Protein abundance distribution (Log_2(protein intensity)) of identified glycoproteins compared with that in the total proteomic data set. (C) Comparison between tumors and the paired NATs using the total intensity of core-fucosylated sites in each sample. (D) Scatterplot depicting comparison of abundance changes between core-fucosylated sites and their corresponding proteins.

Next, the total intensity of core-fucosylated sites was summed in each sample, and it was found that the total intensity of core-fucosylated sites was significantly higher in tumors (p = 0.037) (Figure 3C). Among the 2494 core-fucosylated sites, 1660 sites corresponding to 848 glycoproteins were quantified in at least 50% of samples in tumors (Figure S14). In addition, 690 glycoproteins that contained 1448 core-fucosylated sites were quantified in the proteomic data set. Interestingly, 1208 core-fucosylated sites (83.4%) had greater changes in core fucosylation abundance than those in the corresponding glycoprotein abundance (Figure 3D). These results indicated that the level of core fucosylation upregulated in tumors, which accorded well with the upregulation of FUT8 in tumors (p = 0.019, fold change = 1.86) (Figure S15).

Then, we analyzed aberrant core-fucosylated sites in LUAD. It should be mentioned that the differences of PTM sites could be caused by the changes of either protein abundance or PTM occupation.[39,40] Thus, to identify the relative changes in core-fucosylated sites arising from tumors regardless of total protein levels, we normalized the intensities of core-fucosylated sites to total protein levels (Table S4). After normalization, we observed 196 upregulated and 6 downregulated core-fucosylated sites in tumors relative to paired NATs (p < 0.05 and fold change >1.5) (Figure 4A and Table S5). Further pathway enrichment analysis by the Kyoto Encyclopedia of Genes and Genomes (KEGG) showed that extracellular matrix (ECM)-receptor interaction was significantly enriched by upregulated core fucosylation events (Figure 4B). Remodeling

https://doi.org/10.1021/jacsau.4c00214
JACS Au 2024, 4, 2005−2018

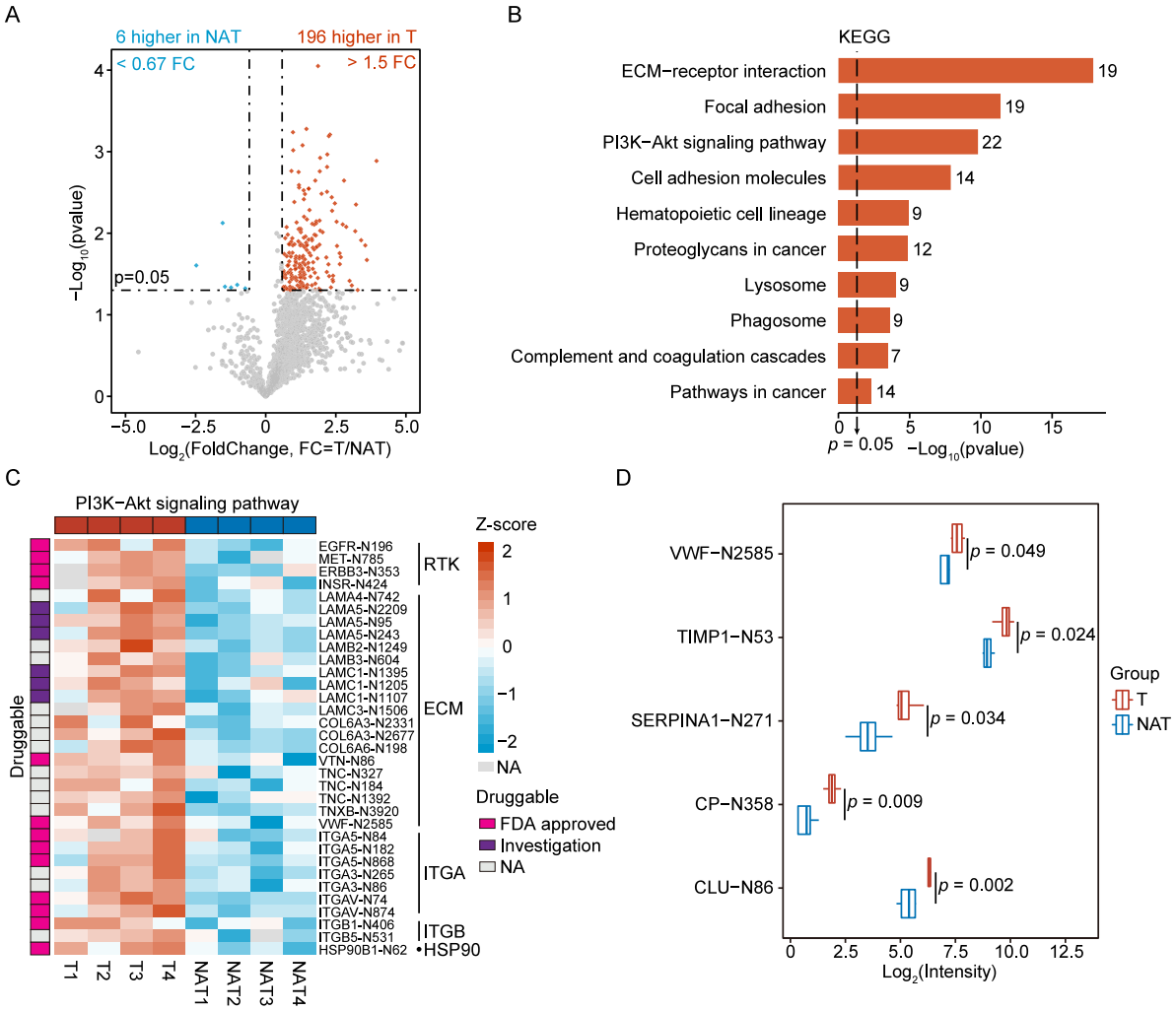

Figure 4. Comparative analysis of the core-fucosylated sites in tumors and the paired NATs. (A) Volcano plot of differentially regulated core-fucosylated sites between tumors and the paired NATs. (B) KEGG analysis of 196 upregulated proteins. (C) Heatmap showing the upregulated sites in the PI3K-Akt signaling pathway. Glycoproteins annotated as drug targets (as defined by https://go.drugbank.com/) are highlighted by vertical bars on the left side of the figure. (D) Box plots showing the relative abundance of upregulated sites in secreted proteins. The *p* value is calculated using student's *t* test.

of the ECM in tumors might be critical to supporting tumorigenesis and tumor progression.[41−43] Besides, upregulated core-fucosylated sites were also associated with the PI3K-Akt signaling pathway (Figures 4B and4C). Hyperactivation of the PI3K-Akt signaling pathway was associated with tumor progression, invasion, metastasis, and poor prognosis.[44−46] Interestingly, we identified 10 putatively druggable glycoproteins with FDA-approved drugs, such as epidermal growth factor receptor (EGFR), mesenchymal-epithelial transition factor (MET), etc. (Table S6). We also identified 2 putatively druggable glycoproteins (laminin alpha5 (LAMA5) and laminin gamma 1 (LAMC1)) with known but as yet non-FDA approved molecules. It was worth noting that most core-fucosylated sites were localized in the extracellular domains of these glycoproteins, which played an important role in mediating the functions of proteins.[47,48] For example, the core-fucosylated site N196 on EGFR and N785 on MET were localized in the extracellular domains that were essential for the activation of EGFR and MET, respectively.[48,49] Furthermore, the core-fucosylated site N196 on EGFR was near the monoclonal antibody (such as cetuximab) binding sites.[50,51] In addition, 73 upregulated core-fucosylated sites were observed on 64 secreted glycoproteins, among which 27 glycoproteins were annotated as plasma proteins (Figure S16). These upregulated core-fucosylated sites might have the potential to serve as biomarkers for early detection of LUAD, e.g., VWF-N2585, TIMP1-N53, SERPINA1-N271, CP-N358, and CLU-N86 (Figure 4D). Taken together, these results suggested that core-fucosylated sites could serve as potential drug development targets and biomarker candidates, although the sample size was limited in this work. A larger cohort and various sample types (e.g., blood plasma) are needed to verify these findings.

Investigating the location and occupation of glycosylated sites on glycoproteins is important for understanding the biological functions of protein glycosylation. Here, our glycosylated probe **1** enabled efficient enrichment of core fucosylation in a "one-step" manner. Compared with previous work, this probe can be used to label cell lysates and human samples.[22] A total of 1200, 1277, and 2494 core-fucosylated sites were identified in H1299, Jurkat, and human LUAD samples using probe **1**, respectively. There are many works on global analysis of core fucosylation events in cancer cell lines and complex human samples. These works mainly employed

https://doi.org/10.1021/jacsau.4c00214
JACS Au 2024, 4, 2005−2018

lectin binding, HILIC, or mixed-mode polymeric sorbent to enrich intact core-fucosylated peptides or glycopeptides, and then EndoF3 was used to simplify these intact glycopeptides.[14,16,18,19] There are also several works identified core-fucosylated sites by chemoenzymatic labeling methods.[22,23,52] On average approximately 500 core-fucosylated sites were identified in cancer cell lines, while about 1000 core-fucosylated sites were detected in complex human samples in these works.[14,16,18,19,22,23,52] Though different cancer cell lines and specimens were used, we were able to identify a total of 1200, 1277, and 2494 core-fucosylated sites in H1299, Jurkat, and human LUAD, indicating the effectiveness and robustness of the current method. However, it is worth mentioning that EndoF3 shows the highest activity only toward core-fucosylated *N*-glycans with bi- and triantennary structures. Hence, this method cannot identify and quantify core-fucosylated sites with more complex *N*-glycan structures, such as tetra-antennary glycan structures.

CONCLUSION

In summary, we have successfully developed a "one-step" strategy for the global analysis of core fucosylation. Taking advantage of the substrate specificity of wild-type EndoF3 and mutant endoglycosidase EndoF3-D165A, a "one-step" probe linked with the PNIPAM polymer can be specifically installed on the core fucose structure without further need for an additional chemical reaction. Owing to the thermosensitive property of PNIPAM, the labeled peptides can be captured from the complex samples. In addition, the traceless cleavage by EndoF3 makes it ideal for the site-specific analysis of core fucosylation by MS technology. The feasibility and effectiveness of our method were evaluated in the BSA spiked with standard core-fucosylated peptides, H1299, and Jurkat cell lines, and it showed a significant improvement over the "two-step" strategy. The "one-step" strategy was further employed to characterize core-fucosylated sites in human LUAD, and 196 upregulated sites were identified in tumors. These upregulated sites might promote the discovery of new drug targets or diagnostic biomarkers. We anticipate that this work will accelerate the study of core fucosylation function in important physiological and pathological processes such as tumorigenesis.

MATERIALS AND METHODS

Materials

All chemical reagents were purchased from commercial sources and used without further purification unless otherwise stated. A poly(*N*-isopropylacrylamide) (PNIPAM) dendrimer (Mn ∼ 10 000) and bovine serum albumin (BSA) were purchased from Sigma-Aldrich. Biotin-PEG_4-alkyne and THPTA were purchased from Click Chemistry Tools. DBCO acid was purchased from Bidepharm (Shanghai, China). Sep-Pak tC18 cartridges were from Waters. Trypsin (0.25% EDTA) was purchased from Yeasen Biotechnology. BCA protein assay kit and streptavidin agarose resin were from Invitrogen. Sequencing grade Modified Trypsin was purchased from Promega. An EDTA-free protease inhibitor cocktail was purchased from New Cell and Molecular (NCM) Biotech. Peptides were purchased from Biochem (Shanghai, China).

Cell Culture

H1299 and Jurkat cells were cultured in the RPMI 1640 medium (Gibco) supplemented with 10% fetal bovine serum and 1% (v/v) penicillin/streptomycin. All cell lines were grown under a humidified atmosphere supplied with 5% CO_2 at 37 °C.

Enzyme Preparation

EndoF3 and EndoF3-D165A from *Elizabethkingia meningoseptica*[53] were synthesized by GenScript (Nanjing, China). All genes were cloned into the pET-28a vector with six histidine tags (6xHis tag) for purification by Ni-affinity chromatography. The confirmed constructs were subsequently transformed into *E. coli* BL21 (DE3) for protein expression. BL21 (DE3) cells harboring a recombinant vector of pET-28a were cultured in 2 L of LB medium containing 50 ug/mL kanamycin in a rotary shaker at 37 °C and 200 rpm, and 0.2 mM IPTG was added until OD was 0.8. Protein expression was allowed to proceed at 16 °C overnight. The cells were harvested by centrifugation at 7000 rpm for 10 min. The cell precipitation was resuspended in lysis buffer (50 mM Tris-HCl buffer, 300 mM NaCl, 10 mM imidazole; pH = 7.5). Cells were disrupted by a microfluidizer, and the lysate was centrifuged at 12 000 g for 10 min to remove the cell debris. The his-tagged proteins were purified using a Ni-NTA agarose column. Before purification, the column was equilibrated with the lysis buffer (50 mM Tris-HCl, 300 mM NaCl, 10 mM imidazole; pH = 7.5). The column was washed with 2 column volumes of the lysis buffer and eluted with elution buffer (50 mM Tris-HCl, 300 mM NaCl, 300 mM imidazole; pH = 7.5). The enzyme was desalted by filtration (Amicon Ultra-5, 10 K_d). Protein concentration was determined by a BCA Protein Assay Kit.

Chemical Synthesis of 1 (Scheme S1)

11-((*tert*-Butoxycarbonyl)amino)undecanoic acid (**6**, 3012 mg, 10 mmol), 2-(7-azabenzotriazol-1-yl)-*N*,*N*,*N*′,*N*′-tetramethyluronium, hexafluorophosphate, (HATU, 7600 mg, 20 mmol), and *N*,*N*-diisopropylethylamine (DIPEA, 5000 μL, 30 mmol) were added to the solution of prop-2-yn-1-amine (825 mg, 15 mmol) in DCM (50 mL). The resulting mixture was stirred at room temperature under a N_2 atmosphere for 4 h. Then, the solvent was removed by rotary evaporation. The solid was purified by dialysis (MWCO 1000) to obtain an alkyne PNIPAM product. the residue was purified by column chromatography on silica gel eluted with DCM/MeOH (50:1−20:1) to give brown oil 7 (2710 mg, yield: 80%). ^{1}H NMR (400 MHz, $CDCl_3$) δ 5.90 (s, 1H), 4.54 (s, 1H), 4.03 (dd, J = 4.7, 2.4 Hz, 2H), 3.07 (t, J = 6.5 Hz, 2H), 2.32−2.06 (m, 3H), 1.66−1.55 (m, 2H), 1.51−1.37 (m, 11H), 1.35−1.15 (m, 12H). ^{13}C NMR (101 MHz, $CDCl_3$) δ: 172.95, 156.14, 79.83, 79.13, 71.55, 40.76, 36.51, 30.14, 29.50, 29.41, 29.33, 29.29, 29.20, 28.54, 26.84, 25.63 (one peak less because of overlapping).

To a solution of compound 7 (2700, 8 mmol) in DCM (10 mL) was added trifluoroacetic acid (TFA, 10 mL), and the resulting mixture was stirred at room temperature for 1 h. After the completion of the reaction (monitored by MS), the solvent was removed by rotary evaporation. The solid was resuspended in Et_2O (50 mL) and filtered. The solid was washed with Et_2O and dried to give white solid **8** (1760 mg, yield: 86%). ^{1}H NMR (400 MHz, DMSO) δ 8.22 (t, J = 5.5 Hz, 1H), 7.62 (s, 2H), 3.82 (dd, J = 5.5, 2.5 Hz, 2H), 3.09 (t, J = 2.5 Hz, 1H), 2.81−2.71 (m, 2H), 2.06 (t, J = 7.4 Hz, 2H), 1.58−1.41 (m, 4H), 1.24 (s, 12H). ^{13}C NMR (101 MHz, DMSO) δ 171.92, 81.41, 72.78, 38.83, 35.05, 28.8, 28.63, 28.52, 27.70, 27.01, 25.78, 25.14 (two peak less because of overlapping).

11 was prepared from the poly(*N*-isopropylacrylamide) (PNIPAM) dendrimer (Mn ∼ 10 000, **9**), amino-alkyne (**8**),

https://doi.org/10.1021/jacsau.4c00214
JACS Au 2024, 4, 2005−2018

and compound **10** according to the reported procedure.[54] Amino-alkyne (**8**, 48 mg, 0.2 mmol), 2-(7-azabenzotriazol-1-yl)-*N*,*N*,*N*′,*N*′-tetramethyluronium, hexafluorophosphate, (HATU, 152 mg, 0.4 mmol), and *N*,*N*-diisopropylethylamine (DIPEA, 105 μL, 0.6 mmol) were added to the solution of compound **9** (1000 mg, 0.1 mmol) in DMF (20 mL). The resulting mixture was stirred at room temperature under a N_2 atmosphere for 8 h. Then, the solvent was removed by rotary evaporation. The solid was resolved by water and purified by dialysis (MWCO ∼ 1000) to obtain an alkyne PNIPAM product. Compound **10** (207 mg, 0.1 mmol), $CuSO_4$ (3.2 mg, 0.02 mmol), L-ascorbic acid sodium salt (VcNa, 19.8 mg, 0.1 mmol), and THPTA (17 mg, 0.04 mmol) were added to the solution of the alkyne PNIPAM compound in DMF (20 mL). The resulting mixture was stirred at room temperature until TLC detection (*i*-PrOH:NH_4OH:H_2O = 7:3:2, v:v:v) indicated the completion of the reaction. The resulting mixture was lyophilized, and the residue was purified by Sephadex G50 (water) to give glycosylated PNIPAM compound **11** (583 mg, yield: 53%). The sugar loading efficiency is about 50% according to the calculation by NMR spectra. The hydrogen at the C1 position on the sugar ring was falling into the signal-silent region. These characteristic peaks were used to calculate loading efficiency and are marked with red asterisks in the spectra.

2-Chloro-1,3-dimethylimidazolinium chloride (DMC, 3.4 mg, 20 μmol) and Et_3N (11 μL, 80 μmol) were added to a solution of compound **11** (45 mg, 2 μmol) in water. The reaction mixture was incubated in an ice bath for 30 min. Then, 4.0 M NaCl in water (100 μL) was added. The temperature of the solution was raised to 40 °C to precipitate compound **1**. After centrifugation (10 000 × g), the oxazoline PNIPAM compound **1** was obtained as a white solid. **1** was used for enrichment without further purification. The hydrogen of the C1 position at 6.06 ppm (double) indicated the formation of the oxazoline ring.

Compounds **2** and **3** were prepared according to the reported work.[23]

The Washing Process

The precipitate was dissolved in water (600 μL) in an ice bath. Then, 4.0 M NaCl in water (200 μL) was added. The mixture's temperature was raised to 40 °C to precipitate the PNIPAM compounds. The solid was collected by centrifugation (10 000 × g).

Enrichment of Standard Peptides (4) with 1

The standard peptide (**4**, 20 μg) was reacted with **1** in the presence of EndoF3-D165A (0.2 mg/mL) in PBS buffer (100 mM, pH = 7.5, 600 μL) at room temperature, and **1** (15 mg) was added every 1 h three times. Then, 4.0 M NaCl in water (200 μL) was added. The mixture's temperature was raised to 40 °C to precipitate the PNIPAM compounds. The supernatant and the solid were separated by centrifugation (10 000 × g). The supernatant was analyzed by HPLC to obtain a decrease of standard peptides (after enrichment with **1**). After three washes (see The Washing Process section), the precipitate was dissolved in a PBS buffer (100 mM, pH = 7.0, 600 μL) in an ice bath. Then, EndoF3 (0.1 mg/mL) were added. The mixture was reacted at room temperature for 12 h. Then, 4.0 M NaCl in water (200 μL) was added. The mixture's temperature was raised to 40 °C to precipitate the PNIPAM compounds. The supernatant was collected by centrifugation (10 000 × g) and analyzed by HPLC to determine the release of standard peptides (release of **1**). The enrichment and release procedure were monitored at 214 nm by reverse phase HPLC. The gradient was set as follows: 10−18% B in 11 min, 18−31% in 9 min.

Enrichment of Standard Peptides (4) with 2 and 3

Reactions were performed in PBS buffer (200 mM, pH = 7.5, 300 μL) containing the standard peptide (**4**, 0.5 mM) and EndoF3-D165A (0.2 mg/mL) at 30 °C. Then, **2** (1 mM) wasadded to the reaction every 30 min five times. Then, the reaction was terminated and analyzed with HPLC to determine the formation of azido-peptides **5** (reacted with **2**). The solution of **5** (corresponding to 20 μg of **4**) was reacted with compound **3** (45 mg) in PBS buffer (100 mM, pH = 7.5, 600 μL) at room temperature for 1 h. Then, 4.0 M NaCl in water (200 μL) was added. The mixture's temperature was raised to 40 °C to precipitate the PNIPAM compounds. The supernatant and the solid were separated by centrifugation (10 000 × g). The supernatant was analyzed by HPLC to obtain the decrease of azido-peptides (after enrichment with **3**). After three washes (see The Washing Process section), the precipitate was dissolved in PBS buffer (100 mM, pH = 7.0, 600 μL) in an ice bath. Then, EndoF3 (0.1 mg/mL) were added. The mixture was reacted at room temperature for 12 h. Then, 4.0 M NaCl in water (200 μL) was added. The mixture's temperature was raised to 40 °C to precipitate the PNIPAM compounds. The supernatant was collected by centrifugation (10 000 × g) and analyzed by HPLC to determine the release of standard peptides (release of **3**). The enrichment and release procedure were monitored at 214 nm by reverse phase HPLC. The gradient was set as follows: 10−18% B in 11 min and 18−31% in 9 min.

Enrichment of the Standard Peptide and BSA Peptide Mixture with 1, 2, and 3

BSA (100 mg) in a NH_4HCO_3 buffer solution (100 mM, 10 mL) was digested with trypsin at 37 °C for 24 h. After the completion of the reaction, the digested peptides were desalted by using a C18 solid-phase column (Sep-Pak tC18 cartridges), lyophilized, and stored at −80 °C for further use. The concentration of digested peptides was determined by the BCA Protein Assay Kit.

Enrichment with 1. The standard peptide (**4**, 20 μg) was mixed with digested BSA peptides (10 mg) in a ratio of 1:500 (w/w). The resulting peptides were reacted with enzymes and **1** (45 mg) according to the procedure described above. Then, 4.0 M NaCl (200 μL) was added. The mixture's temperature was raised to 40 °C to precipitate the PNIPAM compounds. After six washes (see The Washing Process section), the precipitate was dissolved in PBS buffer (100 mM, pH = 7.0, 600 μL) in an ice bath. Then, endoglycosidases (EndoF3, 0.1 mg/mL) were added. The mixture was reacted at room temperature for 12 h. Then, 4.0 M NaCl (200 μL) was added. The temperature of the mixture was raised to 40 °C to precipitate the PNIPAM compounds. The supernatant was collected by centrifugation (10 000 × g). The release of the standard peptides (**4**) in the supernatant was subjected to SDB-RPS solid-phase extraction column desalting (3 M Empore) and analyzed by LC-MS/MS.

Enrichment with 2 and 3. The standard peptide (**4**, 20 μg) was mixed with digested BSA peptides (10 mg) in a ratio of 1:500 (w/w). The resulting peptides were reacted with enzymes and **2** to obtain the azido-peptides according to the procedure described above. The azido-peptides were subjected

https://doi.org/10.1021/jacsau.4c00214
JACS Au 2024, 4, 2005−2018

to C18 solid-phase extraction desalting (Sep-Pak tC18 cartridges) and lyophilized. The azido-peptide solids were dissolved in PBS buffer (100 mM, pH = 7.5, 600 μL) and reacted with alkyne PINPAM compounds (**3**, 45 mg) at room temperature for 1 h. Then, 4.0 M NaCl (200 μL) was added. The mixture's temperature was raised to 40 °C to precipitate the PNIPAM compounds. After six washes (see The Washing Process section), the precipitate was dissolved in PBS buffer (100 mM, pH = 7.0, 600 μL) in an ice bath. Then, endoglycosidases (EndoF3, 0.1 mg/mL) were added. The mixture was reacted at room temperature for 12 h. Then, 4.0 M NaCl (200 μL) was added. The temperature of the mixture was raised to 40 °C to precipitate the PNIPAM compounds. The supernatant was collected by centrifugation (10 000 × g). The release of the standard peptides (**4**) in the supernatant was subjected to SDB-RPS solid-phase extraction column desalting (3 M Empore) and analyzed by LC-MS/MS.

Enrichment of the Cellular Peptides with 1, 2, and 3

Cells were routinely cultured in an RPMI 1640 medium, supplemented with 10% FBS, penicillin (100 U/mL), and streptomycin (100 U/mL) in a humidified cell incubator at 37 °C under an atmosphere of 5% CO_2. The cells were collected and lysed at 4 °C with RIPA lysis buffer (50 mM Tris, 150 mM NaCl, 0.1% (w/v) SDS, and pH 7.4) containing EDTA-free protease inhibitor cocktail (NCM) and 2% SDS for 20 min. The mixture was centrifuged at 4 °C to collect the supernatant. After reduction with dithiothreitol (DTT, 20 mM) at 37 °C for 2 h and alkylation with iodoacetamide (IAA, 40 mM) at 25 °C for 40 min in the dark, proteins were purified and pelleted with the methanol/chloroform/water (4:1:4) precipitation. The protein solid was dissolved and digested with sequencing grade modified trypsin (Promega, enzyme: substrate ratio of ∼1:100) in NH_4HCO_3 buffer (100 mM containing 1 M urea) at 37 °C for 24 h. After digestion, the peptides were subjected to C18 solid-phase extraction desalting (Sep-Pak tC18 cartridges) and lyophilized. The digested peptides (5 mg/mL) were dissolved in PBS buffer (100 mM, pH = 7.5), and EndoF3 (0.1 mg/mL) were added. The mixture was reacted at 37 °C for 2 h. Then, the deglycosylated peptides were subjected to C18 solid-phase extraction desalting (Sep-Pak tC18 cartridges) and lyophilized. The deglycosylated peptides solid were dissolved in water and stored at −80 °C. The concentration of deglycosylated peptides was determined by BCA Protein Assay Kit.

Enrichment with 1. Reactions were performed in PBS buffer (200 mM, pH = 7.5, 300 μL) containing 3 mg of deglycosylated peptides (10 mg/mL) and EndoF3-D165A (0.2 mg/mL) at room temperature. Then, **1** (15 mg) were added to the reaction every 1 h for three times. Then, 4.0 M NaCl (200 μL) was added. The mixture's temperature was raised to 40 °C to precipitate the PNIPAM compounds. The precipitate was collected by centrifugation (10 000 × g). After six washes (see The Washing Process section), the precipitate was dissolved in PBS buffer (100 mM, pH = 7.0, 600 μL) in an ice bath. Then, endoglycosidases (EndoF3, 0.1 mg/mL) were added. The mixture was reacted at room temperature for 12 h. Then, 4.0 M NaCl (200 μL) was added. The mixture's temperature was raised to 40 °C to precipitate the PNIPAM compounds. The glycopeptides in the supernatant were collected by centrifugation (10 000 × g) and lyophilized.

Enrichment with 2 and 3. Reactions were performed in PBS buffer (200 mM, pH = 7.5, 300 μL) containing 3 mg of deglycosylated peptides (10 mg/mL) and EndoF3-D165A (0.2 mg/mL) at room temperature. Then, **2** (1 mM) were added to the reaction every 30 min for five times. Then, the azido-peptides were subjected to C18 solid-phase extraction desalting (Sep-Pak tC18 cartridges) and lyophilized. The azido-peptides were dissolved in PBS buffer (100 mM, pH = 7.5, 600 μL) and reacted with alkyne PINPAM compounds (**3**, 45 mg) at room temperature for 2 h. Then, 4.0 M NaCl (200 μL) was added. The mixture's temperature was raised to 40 °C to precipitate the PNIPAM compounds. The precipitate was collected by centrifugation (10 000 × g). After six washes (see The Washing Process section), the precipitate was dissolved in PBS buffer (100 mM, pH = 7.0, 600 μL) in an ice bath. Then, endoglycosidases (EndoF3, 0.1 mg/mL) were added. The mixture was reacted at room temperature for 12 h. Then, 4.0 M NaCl (200 μL) was added. The mixture's temperature was raised to 40 °C to precipitate the PNIPAM compounds. The glycopeptides in the supernatant were collected by centrifugation (10 000 × g) and lyophilized.

Enrichment of the Human Lung Adenocarcinoma (LUAD) Sample Peptides with 1

Frozen tissues were homogenized in SDT lysis buffer (4% SDS (m/v), 100 mM DTT, 100 mM Tris-HCl, pH = 7.6) (Homogenizer). Then, the proteins were heated at 95 °C for 5 min and centrifuged at 12 000 g for 10 min. The supernatants were collected and the protein concentration was determined by tryptophan fluorescence emission as described previously.[55] After alkylation with IAA (200 mM) at 25 °C for 40 min in the dark, proteins digested with sequencing grade modified trypsin (Promega, enzyme: substrate ratio of ∼1:100) following the solvent precipitation SP3 (SP4) procedure.[56] After digestion, the peptides were subjected to C18 solid-phase extraction desalting (Sep-Pak tC18 cartridges) and lyophilized. A portion of these dried peptides was used for whole proteome analysis.The digested peptides (5 mg/mL) were dissolved in PBS buffer (100 mM, pH = 7.5), and EndoF3 (0.1 mg/mL) were added. The mixture was reacted at 37 °C for 2 h. Then, the deglycosylated peptides were subjected to C18 solid-phase extraction desalting (Sep-Pak tC18 cartridges) and lyophilized. The deglycosylated peptide solids were dissolved in water and stored at −80 °C. The concentration of deglycosylated peptides was determined by the BCA Protein Assay Kit.

Enrichment with 1. Reactions were performed in PBS buffer (200 mM, pH = 7.5, 300 μL) containing 3 mg of deglycosylated peptides (10 mg/mL) and EndoF3-D165A (0.2 mg/mL) at room temperature. Then, **1** (15 mg) were added to the reaction every 1 h for three times. Then, 4.0 M NaCl (200 μL) was added. The mixture's temperature was raised to 40 °C to precipitate the PNIPAM compounds. The precipitate was collected by centrifugation (10 000 × g). After six washes (see The Washing Process section), the precipitate was dissolved in PBS buffer (100 mM, pH = 7.0, 600 μL) in an ice bath. Then, endoglycosidases (EndoF3, 0.1 mg/mL) were added. The mixture was reacted at room temperature for 12 h. Then, 4.0 M NaCl (200 μL) was added. The mixture's temperature was raised to 40 °C to precipitate the PNIPAM compounds. The glycopeptides in the supernatant were collected by centrifugation (10 000 × g) and lyophilized.

Sample Preparation for LC-MS/MS Analysis

The dried glycopeptides were resuspended in 500 μL of 0.1% FA and fractionated with a self-made 10 μm C18 column. Phase A consisted of 10 mM ammonium formate in water (pH

https://doi.org/10.1021/jacsau.4c00214
JACS Au 2024, 4, 2005−2018

= 10.0), and phase B consisted of 10 mM ammonium formate in 90% ACN (pH = 10.0). 2 mg of 10 μm C18 resin were sonicated in ACN and transferred into a 200 μL tip column. The tip column was then sequentially equilibrated with ACN and 0.1% FA. The resuspended glycopeptides were then loaded onto the tip column. The tip column was then washed with 0.1% FA and phase A, respectively. Subsequent fractions were eluted sequentially using 200 μL of 3% phase B/97% phase A (v/v) (1), 6% phase B/94% phase A (v/v) (2), 9% phase B/91% phase A (v/v) (3), 12% phase B/88% phase A (v/v) (4), 15% phase B/85% phase A (v/v) (5), 18% phase B/82% phase A (v/v) (6), 21% phase B/79% phase A (v/v) (7), 25% phase B/75% phase A (v/v) (8), 30% phase B/70% phase A (v/v) (9), 35% phase B/65% phase A (v/v) (10), 50% phase B/50% phase A (v/v) (11), and 100% phase B (12). The fraction (1) was mixed with fraction (7), the fraction (2) was mixed with fraction (8), the fraction (3) was mixed with fraction (9), the fraction (4) was mixed with fraction (10), the fraction (5) was mixed with fraction (11), and the fraction (6) was mixed with fraction (12). These six fractions were evaporated with a Speed Vac. Finally, the fractionated peptides were subjected to a SDB-RPS solid-phase extraction column desalting (3 M Empore).

Nano-LC-MS/MS Data Acquisition for Core-Fucosylated Glycoproteome

The LC-MS/MS analysis was performed using data-dependent acquisition (DDA) on a nanoflow UHPLC nanoElute system (Bruker Daltonics, Germany) coupled with a trapped ion mobility-quadrupole time-of-flight (timsTOF Pro) mass spectrometer (Bruker Daltonics, Germany). The purified peptides were resolved using 0.1% formic acid (FA) in water and separated on an analytical column (75 μm × 20 cm) packed with reverse-phase (RP) beads (1.5 μm ReproSil Saphir C18 beads, 100-Å pore size; Dr. Maisch GmbH, Ammerbuch, Germany) on the nanoElute with a 90 min gradient. The flow rate was set as 250 nL/min from 0 to 85 min and 300 nL/min from 85 to 90 min. The column was heated at 50 °C using a homemade column oven. Buffer A consisted of 0.1% (v/v) FA in water, and buffer B consisted of 0.1% (v/v) FA in 100% ACN. The gradient was set as follows: 2%−4% B in 1 min; 4%−26% B in 77 min; 26%−32% B in 5 min; 32%−90% B in 2 min; 90% B in 5 min.

Data acquisition on the timsTOF Pro was performed using timsControl 4.0.5. The capillary voltage was set to 1500 V. The following parameters were adapted: MS range m/z 100 to 1700 was scanned in positive electrospray mode; the mass spectrometer collected ion mobility MS spectra over $1/k_0$ of 1.51 to 0.60 (V·s)/cm^2, and then performed 10 cycles of parallel accumulation-serial fragmentation (PASEF) MS/MS with a target intensity of 20 000 and a threshold of 2500. The ion accumulation time and ramp time were 100 ms each. The duty cycle was 100%, and total cycle time was 1.17 s. Singly charged precursor ions were excluded with a polygon filter. The collision energy was decreased from 60 eV at $1/k_0$ = 1.50 (V·s)/cm^2 to 54 eV at $1/k_0$ = 1.17 (V·s)/cm^2 to 25 eV at $1/k_0$ = 0.85 (V·s)/cm^2 and end at 20 eV at $1/k_0$ = 0.60 (V·s)/cm^2.

Nano-LC-MS/MS Data Acquisition for LUAD Whole Proteome

The LC-MS/MS analysis was performed using data-independent acquisition (DIA) on a nanoflow UHPLC nanoElute system (Bruker Daltonics, Germany) coupled with a trapped ion mobility-quadrupole time-of-flight (timsTOF Pro) mass spectrometer (Bruker Daltonics, Germany). The purified peptides were resolved using 0.1% FA in water and separated on an analytical column (75 μm × 20 cm) packed with RP beads (1.5 μm ReproSil Saphir C18 beads, 100-Å pore size; Dr. Maisch GmbH, Ammerbuch, Germany) on the nanoElute with a 60 min gradient. The flow rate was set as 300 nL/min at 0−55 min and 300 nL/min at 55−60 min. The column was heated at 50 °C using a homemade column oven. Buffer A consisted of 0.1% (v/v) FA in water, and buffer B consisted of 0.1% (v/v) FA in 100% ACN. The gradient was set as follows: 2%−4% B in 1 min; 4%−26% B in 47 min; 26%−32% B in 5 min; 32%−90% B in 2 min; 90% B in 5 min.

Data acquisition on timsTOF Pro was performed using timsControl 4.0.5. The capillary voltage was set to 1500 V. The following parameters were adapted: the MS range of m/z 100 to 1700 was scanned in positive electrospray mode; the mass spectrometer collected ion mobility MS spectra over $1/k_0$ of 1.29 to 0.76 (V·s)/cm^2. Samples were acquired with a diaPASEF[57] method consisting of 14 cycles, including a total of 28 mass-width windows (25 Da width, from 452 to 1152 Da) with 4 mobility windows each. The ion accumulation time and ramp time were 100 ms each. The duty cycle was 100%, and the total cycle time was 1.59 s.

Database Searching of MS Data

All raw files acquired from LC-MS/MS were analyzed via MaxQuant v2.4.2[32] against the human Swiss-Prot database containing 20 600 sequences (downloaded in June 2021). Carbamidomethyl (cysteine) was selected as a fixed modification, while oxidation (methionine), acetylation (protein N-term), deamidation (asparagine), and fucosyl GlcNAc (asparagine) were set as variable modifications. A maximum number of 5 modifications were allowed for each peptide. Trypsin/P was selected as the digestive enzyme. The maximum missing cleavage site was set as 3, and the minimal peptide length was set at 7. The tolerances of the first search and main search for peptides were set at 20 and 4.5 ppm, respectively. The false discovery rate (FDR) was set to 0.01 at the level of peptides, proteins, and sites.

For LUAD whole proteome, the MS data were analyzed using DIA-NN 1.8 against the human Swiss-Prot database (downloaded in June 2021).[58] Carbamidomethylation (C) was set as a fixed modification, and methionine excision (protein N-terminal) was searched for variable modifications. Trypsin/P was selected as the digestive enzyme with 2 maximum missing cleavages, and the minimal peptide length was set at 7. The false discovery rate (FDR) was set to 0.01 at the level of the peptides and proteins.

Bioinformatic Analysis

Proteins labeled as either contaminants or reverses were removed from analysis. Proteins quantified in at least 50% of all 8 samples in LUAD were included for further analysis. For analysis of differentially expressed core-fucosylated sites, protein-normalized core-fucosylated sites were first calculated by normalizing core-fucosylated sites abundance to their respective protein levels in each sample, and core-fucosylated sites without a matching protein were removed. The cutoff criteria of differentially expressed core-fucosylated sites were set as followings: fold change ≥ 1.50 or ≤ 0.67 and p value < 0.05 (Student's t test).

GO and KEGG enrichment was performed by Database for Annotation, Visualization, and Integrated Discovery (DAVID, https://david.ncifcrf.gov/).[59] Sequence motif analysis was

https://doi.org/10.1021/jacsau.4c00214
JACS Au 2024, 4, 2005−2018

carried out using the R package "ggseqlogo."[60] Hierarchical clustering heatmaps were performed using the R package "ComplexHeatmap." Other visualizations not specifically indicated were performed using the R package "ggplot2."

■ ASSOCIATED CONTENT

Data Availability Statement

The mass spectrometry proteomics data have been deposited to the integrated proteome resources (iProX) (https://www.iprox.cn/) via the PRIDE partner repository with the identifier PXD051139 or IPX0007703000.[61,62]

Supporting Information

The Supporting Information is available free of charge at https://pubs.acs.org/doi/10.1021/jacsau.4c00214.

Chemical synthesis of **1** (Scheme S1); NMR spectra of probe **1** in D_2O (Figure S1); chromatograms of LC−MS analysis of the glycopeptide (**4**) and BSA peptide mixture (Figure S2); core-fucosylated sites identified by the "two-step" (probes**2** and **3**) method in H1299 cells and Jurkat cells (Figures S3 and S5); core-fucosylated sites identified by the "one-step" (probe **1**) method in Jurkat cells (Figure S4); identified core-fucosylated sites in H1299 and Jurkat in this work (Figure S6); GOBP, GOCC, GOMF, and KEGG analysis of the identified 671 proteins containing core-fucosylated sites from H1299 cells (Figure S7); GOBP, GOCC, GOMF, and KEGG analysis of the identified 722 proteins containing core-fucosylated sites from Jurkat cells (Figure S8); domain analysis of the identified core-fucosylated proteins (Figure S9); landscape distribution of the overlapped core-fucosylated sites in H1299 and Jurkat cells and its frequency in proteins (Figure S10); core-fucosylated sites identified by the "one-step" (probe **1**) method in LUAD (Figure S11); GOBP, GOCC, GOMF, and KEGG analysis of the identified 1176 proteins containing core-fucosylated sites from human samples (Figure S12); core-fucosylated sites identified by the "one-step" (probe **1**) method in this work (Figure S13); entire process for differentially regulated core-fucosylated sites screening (Figure S14); boxplots showing the relative abundance of FUT8 in tumors and NATs (Figure S15); heatmap showing the upregulated sites in secreted proteins (Figure S16) (PDF)

Potential core-fucosylated sites identified in H1299 (Table S1) (XLSX)

Potential core-fucosylated sites identified in Jurkat (Table S2) (XLSX)

Overlap of the core-fucosylated sites in H1299 and Jurkat (Table S3) (XLSX)

Identified and quantified core-fucosylated sites in LUAD (Table S4) (XLSX)

Upregulated core-fucosylated sites in LUAD (Table S5) (XLSX)

Identified druggable glycoproteins and corresponding drugs (Table S6) (XLSX)

■ AUTHOR INFORMATION

Corresponding Authors

Yinping Tian − *Carbohydrate-Based Drug Research Center, State Key Laboratory of Chemical Biology, Shanghai Institute of Materia Medica, Chinese Academy of Sciences, Shanghai 201203, China;* orcid.org/0000-0002-6998-0612; Email: tianyinping@simm.ac.cn

Liuqing Wen − *Carbohydrate-Based Drug Research Center, State Key Laboratory of Chemical Biology, Shanghai Institute of Materia Medica, Chinese Academy of Sciences, Shanghai 201203, China; School of Chinese Materia Medica, Nanjing University of Chinese Medicine, Nanjing 210023, China; University of Chinese Academy of Sciences, Beijing 100049, China;* orcid.org/0000-0001-9187-7999; Email: lwen@simm.ac.cn

Hu Zhou − *School of Pharmaceutical Science and Technology, Hangzhou Institute for Advanced Study, University of Chinese Academy of Sciences, Hangzhou 310024, China; Department of Analytical Chemistry, State Key Laboratory of Drug Research, Shanghai Institute of Materia Medica, Chinese Academy of Sciences, Shanghai 201203, China; School of Chinese Materia Medica, Nanjing University of Chinese Medicine, Nanjing 210023, China; University of Chinese Academy of Sciences, Beijing 100049, China;* orcid.org/0000-0001-7006-4737; Email: zhouhu@simm.ac.cn

Authors

Yuqiu Wang − *Department of Otolaryngology, Eye & ENT Hospital, Fudan University, Shanghai 200031, China; Department of Analytical Chemistry, State Key Laboratory of Drug Research, Shanghai Institute of Materia Medica, Chinese Academy of Sciences, Shanghai 201203, China;* orcid.org/0009-0001-8931-8853

Rui Yuan − *School of Chinese Materia Medica, Nanjing University of Chinese Medicine, Nanjing 210023, China*

Bo Liang − *Department of Hematology, Xinxiang Central Hospital, Xinxiang 453000, China*

Jing Zhang − *Department of Thoracic Surgery, Shanghai Pulmonary Hospital, School of Medicine, Tongji University, Shanghai 200433, China*

Qin Wen − *School of Chinese Materia Medica, Nanjing University of Chinese Medicine, Nanjing 210023, China*

Hongxu Chen − *School of Chinese Materia Medica, Nanjing University of Chinese Medicine, Nanjing 210023, China*

Complete contact information is available at: https://pubs.acs.org/10.1021/jacsau.4c00214

Author Contributions

◆Y.W., R.Y., and B.L. contributed equally to this work. CRediT: **Yuqiu Wang** data curation, formal analysis, investigation, resources, software, visualization, writing-original draft, writing-review & editing; **Rui Yuan** data curation, investigation, methodology, writing-review & editing; **Bo Liang** investigation, methodology, resources; **Jing Zhang** investigation, resources; **Qin Wen** investigation, methodology; **Hongxu Chen** data curation, investigation, methodology; **Yinping Tian** investigation, methodology, supervision, writing-original draft, writing-review & editing; **Liuqing Wen** conceptualization, funding acquisition, project administration, supervision, validation, writing-review & editing; **Hu Zhou** conceptualization, funding acquisition, project administration, supervision, writing-review & editing.

Notes

The authors declare no competing financial interest.

https://doi.org/10.1021/jacsau.4c00214
JACS Au 2024, 4, 2005−2018

■ ACKNOWLEDGMENTS

This work was financially supported by the National Key Research and Development Program (2022YFA1302902 to H.Z.), the National Natural Science Foundation of China (22007092 to L.W. and 22307127 to Y.T.), the China Postdoctoral Science Foundation (GZB20230157 to Y.W.), and the Shanghai Municipal Science and Technology Major Project. The study was approved by the Research Ethics Committee of Shanghai Pulmonary Hospital, and written informed consent was obtained from each patient. We would like to thank the Institutional Technology Service Center of Shanghai Institute of Materia Medica for all the technical support.

■ REFERENCES

(1) Eichler, J. Protein glycosylation. *Curr. Biol.* **2019**, *29* (7), R229−R231.
(2) Wolfert, M. A.; Boons, G. J. Adaptive immune activation: glycosylation does matter. *Nat. Chem. Biol.* **2013**, *9* (12), 776−784.
(3) Acs, A.; Ozohanics, O.; Vekey, K.; Drahos, L.; Turiak, L. Distinguishing Core and Antenna Fucosylated Glycopeptides Based on Low-Energy Tandem Mass Spectra. *Anal. Chem.* **2018**, *90* (21), 12776−12782.
(4) Garcia-Garcia, A.; Serna, S.; Yang, Z.; Delso, I.; Taleb, V.; Hicks, T.; Artschwager, R.; Vakhrushev, S. Y.; Clausen, H.; Angulo, J.; et al.et al. FUT8-Directed Core Fucosylation of N-glycans Is Regulated by the Glycan Structure and Protein Environment. *ACS Catal.* **2021**, *11* (15), 9052−9065.
(5) Antonarelli, G.; Pieri, V.; Porta, F. M.; Fusco, N.; Finocchiaro, G.; Curigliano, G.; Criscitiello, C. Targeting Post-Translational Modifications to Improve Combinatorial Therapies in Breast Cancer: The Role of Fucosylation. *Cells* **2023**, *12*, 840.
(6) Comunale, M. A.; Lowman, M.; Long, R. E.; Krakover, J.; Philip, R.; Seeholzer, S.; Evans, A. A.; Hann, H. W.; Block, T. M.; Mehta, A. S. Proteomic analysis of serum associated fucosylated glycoproteins in the development of primary hepatocellular carcinoma. *J. Proteome Res.* **2006**, *5* (2), 308−315.
(7) Chen, C. Y.; Jan, Y. H.; Juan, Y. H.; Yang, C. J.; Huang, M. S.; Yu, C. J.; Yang, P. C.; Hsiao, M.; Hsu, T. L.; Wong, C. H. Fucosyltransferase 8 as a functional regulator of nonsmall cell lung cancer. *P. Natl. Acad. Sci. U.S.A.* **2013**, *110* (2), 630−635.
(8) Liang, C.; Fukuda, T.; Isaji, T.; Duan, C.; Song, W.; Wang, Y.; Gu, J. alpha1,6-Fucosyltransferase contributes to cell migration and proliferation as well as to cancer stemness features in pancreatic carcinoma. *Biochim. Biophys. Acta, Gen. Subj.* **2021**, *1865* (6), 129870.
(9) Pieri, V.; Gallotti, A. L.; Drago, D.; Cominelli, M.; Pagano, I.; Conti, V.; Valtorta, S.; Coliva, A.; Lago, S.; Michelatti, D.; et al.et al. Aberrant L-Fucose Accumulation and Increased Core Fucosylation Are Metabolic Liabilities in Mesenchymal Glioblastoma. *Cancer Res.* **2023**, *83* (2), 195−218.
(10) Agrawal, P.; Fontanals, B.; Sokolova, E.; Jacob, S.; Vaiana, C. A.; McDermott, M.; Argibay, D.; Darvishian, F.; Castillo, M.; Ueberheide, B.; Osman, I.; Fenyo, D.; Mahal, L. K.; Hernando, E. A systems biology approach identifies FUT8 as a novel driver of melanoma metastasis. *Glycobiology* **2016**, *26* (12), 1447−1448.
(11) Liao, C.; An, J.; Yi, S.; Tan, Z.; Wang, H.; Li, H.; Guan, X.; Liu, J.; Wang, Q. FUT8 and Protein Core Fucosylation in Tumours: From Diagnosis to Treatment. *J. Cancer* **2021**, *12* (13), 4109−4120.
(12) Nouso, K.; Kobayashi, Y.; Nakamura, S.; Kobayashi, S.; Takayama, H.; Toshimori, J.; Kuwaki, K.; Hagihara, H.; Onishi, H.; Miyake, Y.; et al.et al. Prognostic importance of fucosylated alpha-fetoprotein in hepatocellular carcinoma patients with low alpha-fetoprotein. *J. Gastroen Hepatol.* **2011**, *26* (7), 1195−1200.
(13) Pan, Q.; Xie, Y.; Zhang, Y.; Guo, X.; Wang, J.; Liu, M.; Zhang, X.-L. EGFR core fucosylation, induced by hepatitis C virus, promotes TRIM40-mediated-RIG-I ubiquitination and suppresses interferon-I antiviral defenses. *Nat. Commun.* **2024**, *15* (1), 652.
(14) Ma, C.; Zhang, Q.; Qu, J. Y.; Zhao, X. Y.; Li, X.; Liu, Y. P.; Wang, P. G. A precise approach in large scale core-fucosylated glycoprotein identification with low- and high-normalized collision energy. *J. Proteomics* **2015**, *114*, 61−70.
(15) Tan, Z.; Yin, H.; Nie, S.; Lin, Z.; Zhu, J.; Ruffin, M. T.; Anderson, M. A.; Simeone, D. M.; Lubman, D. M. Large-scale identification of core-fucosylated glycopeptide sites in pancreatic cancer serum using mass spectrometry. *J. Proteome Res.* **2015**, *14* (4), 1968−1978.
(16) Zhao, X.; Yu, Z.; Huang, Y.; Liu, C.; Wang, M.; Li, X.; Qan, X.; Ying, W. Integrated Strategy for Large-Scale Investigation on Protein Core Fucosylation Stoichiometry Based on Glycan-Simplification and Paired-Peaks-Extraction. *Anal. Chem.* **2020**, *92* (4), 2896−2901.
(17) Cao, Q. C.; Zhao, X. Y.; Zhao, Q.; Lv, X. D.; Ma, C.; Li, X. Y.; Zhao, Y.; Peng, B.; Ying, W. T.; Qian, X. H. Strategy Integrating Stepped Fragmentation and Glycan Diagnostic Ion-Based Spectrum Refinement for the Identification of Core Fucosylated Glycoproteome Using Mass Spectrometry. *Anal. Chem.* **2014**, *86* (14), 6804−6811.
(18) Zhou, J. L.; Yang, W. M.; Hu, Y. W.; Höti, N.; Liu, Y.; Shah, P.; Sun, S. S.; Clark, D.; Thomas, S.; Zhang, H. Site-Specific Fucosylation Analysis Identifying Glycoproteins Associated with Aggressive Prostate Cancer Cell Lines Using Tandem Affinity Enrichments of Intact Glycopeptides Followed by Mass Spectrometry. *Anal. Chem.* **2017**, *89* (14), 7623−7630.
(19) Cao, L. W.; Lih, T. M.; Hu, Y.; Schnaubelt, M.; Chen, S.-Y.; Zhou, Y.; Guo, C.; Dong, M.; Yang, W.; Eguez, R. V.; Chen, L.; Clark, D. J.; Sodhi, A.; Li, Q.; Zhang, H. Characterization of core fucosylation via sequential enzymatic treatments of intact glycopeptides and mass spectrometry analysis. *Nat. Commun.* **2022**, *13* (1), 3910.
(20) Kizuka, Y.; Funayama, S.; Shogomori, H.; Nakano, M.; Nakajima, K.; Oka, R.; Kitazume, S.; Yamaguchi, Y.; Sano, M.; Korekane, H.; et al.et al. High-Sensitivity and Low-Toxicity Fucose Probe for Glycan Imaging and Biomarker Discovery. *Cell Chem. Biol.* **2016**, *23* (7), 782−792.
(21) Chuh, K. N.; Batt, A. R.; Pratt, M. R. Chemical Methods for Encoding and Decoding of Posttranslational Modifications. *Cell Chem. Biol.* **2016**, *23* (1), 86−107.
(22) Tian, Y.; Wang, Y.; Yin, H.; Luo, Y.; Wei, F.; Zhou, H.; Wen, L. A Sensitive and Reversible Labeling Strategy Enables Global Mapping of the Core-Fucosylated Glycoproteome on Cell Surfaces. *Angew. Chem., Int. Ed.* **2022**, *61* (49), No. e202206802.
(23) Luo, Y. W.; Wang, Y. Q.; Tian, Y. P.; Zhou, H.; Wen, L. Q. "Two Birds One Stone" Strategy for the Site-Specific Analysis of Core Fucosylation and *O*-GlcNAcylation. *J. Am. Chem. Soc.* **2023**, *145* (29), 15879−15887.
(24) Ruben, L. C.; Laura, M. R.; Almudena, F. B.; Emilio, G. M. Glycan array analysis of Pholiota squarrosa lectin and other fucose-oriented lectins. *Glycobiology* **2021**, *31* (4), 459−476.
(25) Tang, F.; Zhou, M.; Qin, K.; Shi, W.; Yashinov, A.; Yang, Y.; Yang, L.; Guan, D.; Zhao, L.; Tang, Y.; et al.et al. Selective N-glycan editing on living cell surfaces to probe glycoconjugate function. *Nat. Chem. Biol.* **2020**, *16* (7), 766−775.
(26) Wen, L. Q.; Gadi, M. R.; Zheng, Y.; Gibbons, C.; Kondengaden, S. M.; Zhang, J. B.; Wang, P. G. Chemoenzymatic Synthesis of Unnatural Nucleotide Sugars for Enzymatic Bioorthogonal Labeling. *ACS Catal.* **2018**, *8* (8), 7659−7666.
(27) Wen, L.; Liu, D.; Zheng, Y.; Huang, K.; Cao, X.; Song, J.; Wang, P. G. A One-Step Chemoenzymatic Labeling Strategy for Probing Sialylated Thomsen-Friedenreich Antigen. *ACS Cent. Sci.* **2018**, *4* (4), 451−457.
(28) Tian, Y.; Zhu, Q.; Sun, Z.; Geng, D.; Lin, B.; Su, X.; He, J.; Guo, M.; Xu, H.; Zhao, Y.; et al.et al. One-Step Enzymatic Labeling Reveals a Critical Role of O-GlcNAcylation in Cell-Cycle Progression and DNA Damage Response. *Angew. Chem., Int. Ed. Engl.* **2021**, *60* (50), 26128−26135.
(29) Sun, T.; Yu, S. H.; Zhao, P.; Meng, L.; Moremen, K. W.; Wells, L.; Steet, R.; Boons, G. J. One-Step Selective Exoenzymatic Labeling (SEEL) Strategy for the Biotinylation and Identification of

https://doi.org/10.1021/jacsau.4c00214
JACS Au 2024, 4, 2005−2018

Glycoproteins of Living Cells. *J. Am. Chem. Soc.* **2016**, *138* (36), 11575−11582.
(30) Zhang, J. B.; Chen, C. C.; Gadi, M. R.; Gibbons, C.; Guo, Y. X.; Cao, X. F.; Edmunds, G.; Wang, S. S.; Liu, D.; Yu, J.; et al.et al. Machine-Driven Enzymatic Oligosaccharide Synthesis by Using a Peptide Synthesizer. *Angew. Chem., Int. Ed.* **2018**, *57* (51), 16638−16642.
(31) Huang, X. F.; Witte, K. L.; Bergbreiter, D. E.; Wong, C. H. Homogenous enzymatic synthesis using a thermo-responsive water-soluble polymer support. *Adv. Synth. Catal.* **2001**, *343* (6−7), 675−681.
(32) Cox, J.; Mann, M. MaxQuant enables high peptide identification rates, individualized p.p.b.-range mass accuracies and proteome-wide protein quantification. *Nat. Biotechnol.* **2008**, *26* (12), 1367−1372.
(33) Zielinska, D. F.; Gnad, F.; Wisniewski, J. R.; Mann, M. Precision Mapping of an In Vivo N-Glycoproteome Reveals Rigid Topological and Sequence Constraints. *Cell* **2010**, *141* (5), 897−907.
(34) He, L.; Guo, Z.; Wang, W.; Tian, S.; Lin, R. FUT2 inhibits the EMT and metastasis of colorectal cancer by increasing LRP1 fucosylation. *Cell Commun. Signaling* **2023**, *21* (1), 63.
(35) Martin-Kleiner, I.; Troselj, K. G. Mannose-6-phosphate/insulin-like growth factor 2 receptor (M6P/IGF2R) in carcinogenesis. *Cancer Lett.* **2010**, *289* (1), 11−22.
(36) Gavel, Y.; Heijne, G. V. Sequence differences between glycosylated and non-glycosylated Asn-X-Thr/Ser acceptor sites: implications for protein engineering. *Protein Eng.* **1990**, *3* (5), 433−442.
(37) Nilsson, I.; von Heijne, G. Glycosylation efficiency of Asn-Xaa-Thr sequons depends both on the distance from the C terminus and on the presence of a downstream transmembrane segment. *J. Biol. Chem.* **2000**, *275* (23), 17338−17343.
(38) Gillette, M. A.; Satpathy, S.; Cao, S.; Dhanasekaran, S. M.; Vasaikar, S. V.; Krug, K.; Petralia, F.; Li, Y. Z.; Liang, W. W.; Reva, B.; Krek, A.; Ji, J. Y.; Song, X. Y.; Liu, W. K.; Hong, R. Y.; Yao, L. J.; Blumenberg, L.; Savage, S. R.; Wendl, M. C.; Wen, B.; Li, K.; Tang, L. C.; MacMullan, M. A.; Avanessian, S. C.; Kane, M. H.; Newton, C. J.; Cornwell, M.; Kothadia, R. B.; Ma, W. P.; Yoo, S.; Mannan, R.; Vats, P.; Kumar-Sinha, C.; Kawaler, E. A.; Omelchenko, T.; Colaprico, A.; Geffen, Y.; Maruvka, Y. E.; Leprevost, F. D.; Wiznerowicz, M.; Gümüs, Z. H.; Veluswamy, R. R.; Hostetter, G.; Heiman, D.; Wyczalkowski, M. A.; Hiltke, T.; Mesri, M.; Kinsinger, C. R.; Boja, E. S.; Omenn, G. S.; Chinnaiyan, A. M.; Rodriguez, H.; Li, Q. K.; Jewell, S. D.; Thiagarajan, M.; Getz, G.; Zhang, B.; Fenyö, D.; Ruggles, K.; Cieslik, M. P.; Robles, A.; Clauser, K. R.; Govindan, R.; Wang, P.; Nesvizhskii, A.; Ding, L.; Mani, D. R.; Carr, S. A.; Cons, C. P. T. A. Proteogenomic Characterization Reveals Therapeutic Vulnerabilities in Lung Adenocarcinoma. *Cell* **2020**, *182* (1), 200−225.e35.
(39) Chen, Y. J.; Roumeliotis, T.; Chang, Y. H.; Chen, C. T.; Han, C. L.; Lin, M. H.; Chen, H. W.; Chang, G. C.; Chang, Y. L.; Wu, C. T.; et al.et.al Proteogenomics of Non-smoking Lung Cancer in East Asia Delineates Molecular Signatures of Pathogenesis and Progression. *Cell* **2020**, *182* (1), 226−244.e17.
(40) Wang, Y. Q.; Li, J. M.; Lu, D. Y.; Meng, Q.; Song, N. X.; Zhou, H.; Xiao, X.; Sun, L. M.; Zhu, H. W. Integrated proteome and phosphoproteome analysis of interscapular brown adipose and subcutaneous white adipose tissues upon high fat diet feeding in mouse. *J. Proteomics.* **2022**, *255*, 104500.
(41) Winkler, J.; Abisoye-Ogunniyan, A.; Metcalf, K. J.; Werb, Z. Concepts of extracellular matrix remodelling in tumour progression and metastasis. *Nat. Commun.* **2020**, *11* (1), 5120.
(42) Tian, C. X.; Clauser, K. R.; Öhlund, D.; Rickelt, S.; Huang, Y.; Gupta, M.; Mani, D. R.; Carr, S. A.; Tuveson, D. A.; Hynes, R. O. Proteomic analyses of ECM during pancreatic ductal adenocarcinoma progression reveal different contributions by tumor and stromal cells. *P. Natl. Acad. Sci. U.S.A.* **2019**, *116* (39), 19609−19618.
(43) Huang, J.; Zhang, L.; Wan, D.; Zhou, L.; Zheng, S.; Lin, S.; Qiao, Y. Extracellular matrix and its therapeutic potential for cancer treatment. *Signal Transduct. Target. Ther.* **2021**, *6* (1), 153.
(44) Toulany, M.; Rodemann, H. P. Phosphatidylinositol 3-kinase/Akt signaling as a key mediator of tumor cell responsiveness to radiation. *Semin Cancer Biol.* **2015**, *35*, 180−190.
(45) Fresno Vara, J. A.; Casado, E.; de Castro, J.; Cejas, P.; Belda-Iniesta, C.; Gonzalez-Baron, M. PI3K/Akt signalling pathway and cancer. *Cancer Treat Rev.* **2004**, *30* (2), 193−204.
(46) Torres-Arzayus, M. I.; Font de Mora, J.; Yuan, J.; Vazquez, F.; Bronson, R.; Rue, M.; Sellers, W. R.; Brown, M. High tumor incidence and activation of the PI3K/AKT pathway in transgenic mice define AIB1 as an oncogene. *Cancer Cell* **2004**, *6* (3), 263−274.
(47) Liang, K. H.; Tso, H. C.; Hung, S. H.; Kuan, I. I.; Lai, J. K.; Ke, F. Y.; Chuang, Y. T.; Liu, I. J.; Wang, Y. P.; Chen, R. H.; et al.etal. Extracellular domain of EpCAM enhances tumor progression through EGFR signaling in colon cancer cells. *Cancer Lett.* **2018**, *433*, 165−175.
(48) Hussain, M. R. M.; Iqbal, Z.; Qazi, W. M.; Hoessli, D. C. Charge and Polarity Preferences for N-Glycosylation: A Genome-Wide In Silico Study and Its Implications Regarding Constitutive Proliferation and Adhesion of Carcinoma Cells. *Front. Oncol.* **2018**, *8*, 29.
(49) Han, R.; Lin, C.; Lu, C.; Wang, Y.; Kang, J.; Hu, C.; Dou, Y.; Wu, D.; He, T.; Tang, H.; et al.et al. Sialyltransferase ST3GAL4 confers osimertinib resistance and offers strategies to overcome resistance in non-small cell lung cancer. *Cancer Lett.* **2024**, *588*, 216762.
(50) Li, S.; Schmitz, K. R.; Jeffrey, P. D.; Wiltzius, J. J.; Kussie, P.; Ferguson, K. M. Structural basis for inhibition of the epidermal growth factor receptor by cetuximab. *Cancer Cell* **2005**, *7* (4), 301−311.
(51) Harari, P. M. Epidermal growth factor receptor inhibition strategies in oncology. *Endocr Relat Cancer* **2004**, *11* (4), 689−708.
(52) Li, H.; Li, L.; Cheng, K.; Ning, Z.; Mayne, J.; Zhang, X.; Walker, K.; Chen, R.; Twine, S.; Li, J.; et al.et al. Chemoenzymatic Method for Glycoproteomic N-Glycan Type Quantitation. *Anal. Chem.* **2020**, *92* (1), 1618−1627.
(53) Huang, W.; Li, J.; Wang, L.-X. Unusual Transglycosylation Activity of Flavobacterium meningosepticum Endoglycosidases Enables Convergent Chemoenzymatic Synthesis of Core Fucosylated Complex N-Glycopeptides. *ChemBiochem* **2011**, *12* (6), 932−941.
(54) Tang, F.; Wang, L. X.; Huang, W. Chemoenzymatic synthesis of glycoengineered IgG antibodies and glycosite-specific antibody-drug conjugates. *Nat. Protoc.* **2017**, *12* (8), 1702−1721.
(55) Kulak, N. A.; Pichler, G.; Paron, I.; Nagaraj, N.; Mann, M. Minimal, encapsulated proteomic-sample processing applied to copy-number estimation in eukaryotic cells. *Nat. Methods* **2014**, *11* (3), 319−U300.
(56) Johnston, H. E.; Yadav, K.; Kirkpatrick, J. M.; Biggs, G. S.; Oxley, D.; Kramer, H. B.; Samant, R. S. Solvent Precipitation SP3 (SP4) Enhances Recovery for Proteomics Sample Preparation without Magnetic Beads. *Anal. Chem.* **2022**, *94* (29), 10320−10328.
(57) Meier, F.; Brunner, A. D.; Frank, M.; Ha, A.; Bludau, I.; Voytik, E.; Kaspar-Schoenefeld, S.; Lubeck, M.; Raether, O.; Bache, N.; et al.etal. diaPASEF: parallel accumulation-serial fragmentation combined with data-independent acquisition. *Nat. Methods* **2020**, *17* (12), 1229−1236.
(58) Demichev, V.; Messner, C. B.; Vernardis, S. I.; Lilley, K. S.; Ralser, M. DIA-NN: neural networks and interference correction enable deep proteome coverage in high throughput. *Nat. Methods* **2020**, *17* (1), 41−44.
(59) Huang, D. W.; Sherman, B. T.; Lempicki, R. A. Systematic and integrative analysis of large gene lists using DAVID bioinformatics resources. *Nat. Protoc.* **2009**, *4* (1), 44−57.
(60) Wagih, O. ggseqlogo: a versatile R package for drawing sequence logos. *Bioinformatics* **2017**, *33* (22), 3645−3647.
(61) Ma, J.; Chen, T.; Wu, S.; Yang, C.; Bai, M.; Shu, K.; Li, K.; Zhang, G.; Jin, Z.; He, F.; et al.et al. iProX: an integrated proteome resource. *Nucleic Acids Res.* **2019**, *47* (D1), D1211−D1217.
(62) Vizcaino, J. A.; Cote, R. G.; Csordas, A.; Dianes, J. A.; Fabregat, A.; Foster, J. M.; Griss, J.; Alpi, E.; Birim, M.; Contell, J.; O'Kelly, G.;

https://doi.org/10.1021/jacsau.4c00214
JACS Au 2024, 4, 2005−2018

Schoenegger, A.; Ovelleiro, D.; Perez-Riverol, Y.; Reisinger, F.; Rios, D.; Wang, R.; Hermjakob, H. The PRoteomics IDEntifications (PRIDE) database and associated tools: status in 2013. *Nucleic Acids Res.* **2013**, *41* (D1), D1063−D1069.

https://doi.org/10.1021/jacsau.4c00214
JACS Au 2024, 4, 2005−2018